Supplement of The Cryosphere, 16, 2859–2879, 2022
https://doi.org/10.5194/tc-16-2859-2022-supplement

The Cryosphere Open Access EGU

Supplement of

Coherent backscatter enhancement in bistatic Ku- and X-band radar observations of dry snow

Marcel Stefko et al.

Correspondence to: Marcel Stefko (stefko@ifu.baug.ethz.ch) and Silvan Leinss (leinss@gamma-rs.ch)

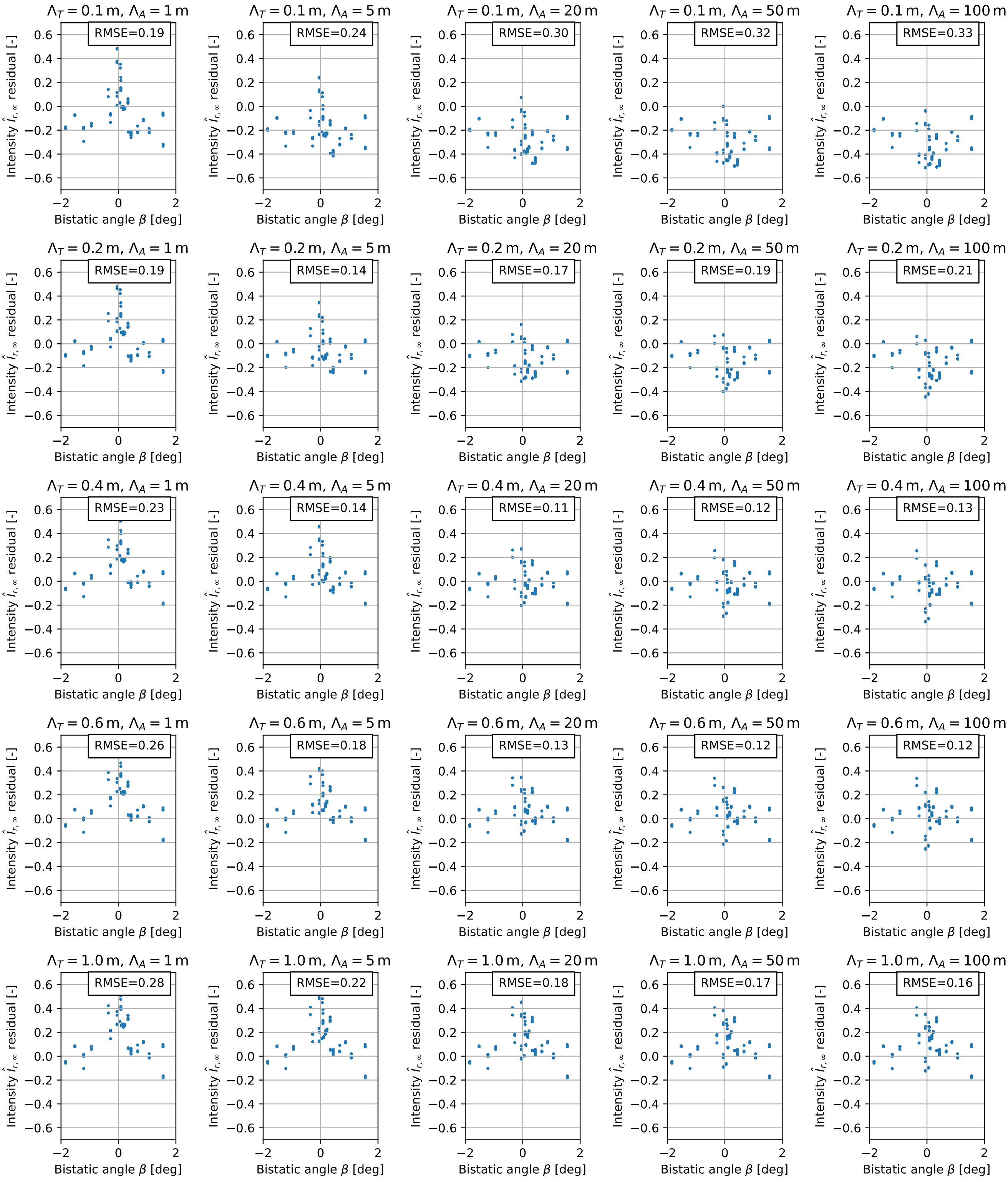

Figure S1. Plots of residuals of winter KAPRI measurements at Davos, Rinerhorn, in the VV polarimetric channel, with varying values of model parameters Λ_T (constant along rows) and Λ_A (constant along columns). The residual was computed as the difference between observed value of $\hat{I}_{\mathrm{r},\infty}$ and value predicted by the model $I_{\mathrm{r},\infty}$ defined by parameters Λ_T, Λ_A, at the corresponding bistatic angle β.

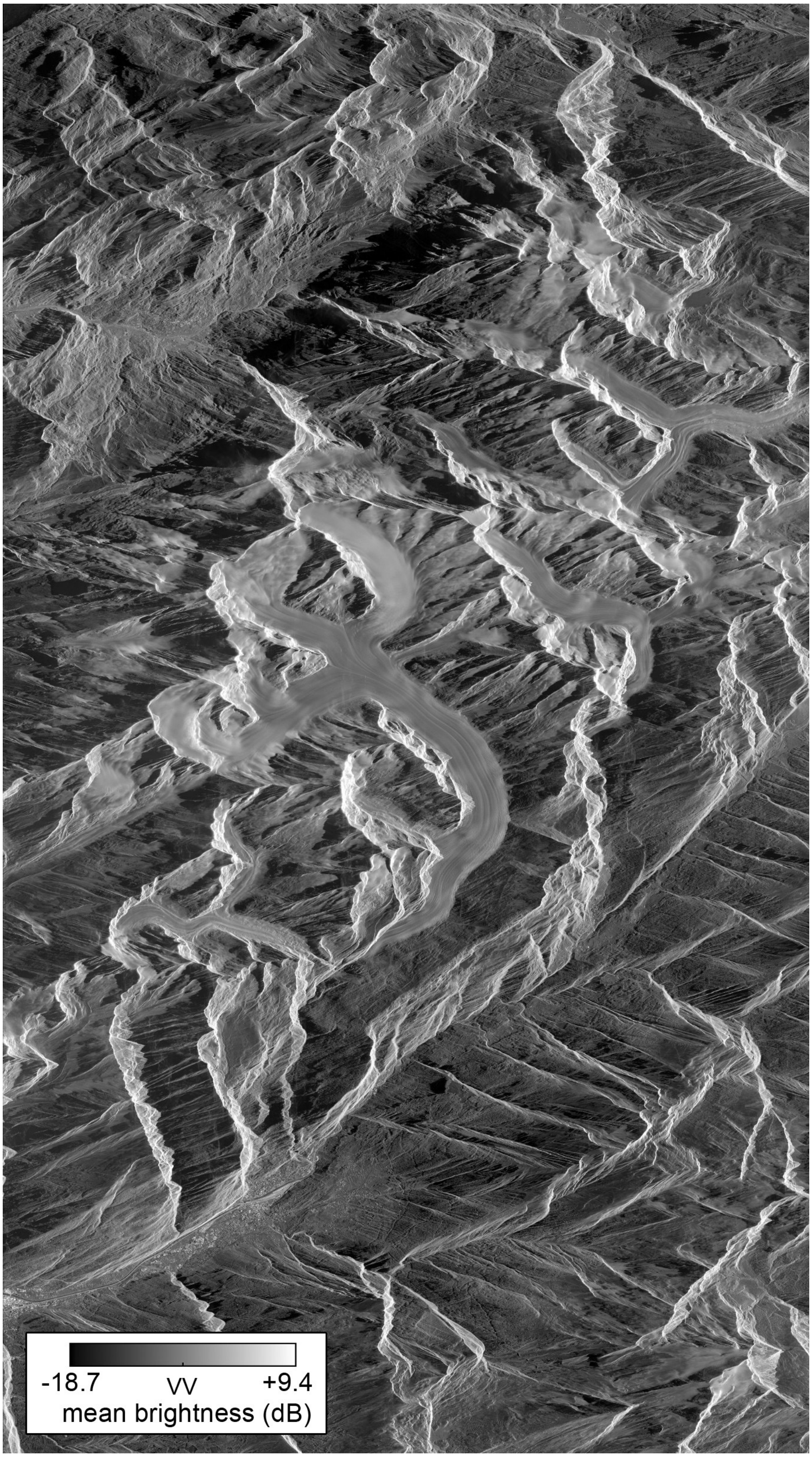

Figure S2. Intensity average of 118 TanDEM-X acquisitions of the Jungfrau-Aletsch region (VV polarization). The image has been flipped/rotated to align approximately with the north-direction. The slant-range direction is from right to left; azimuth from top to bottom.

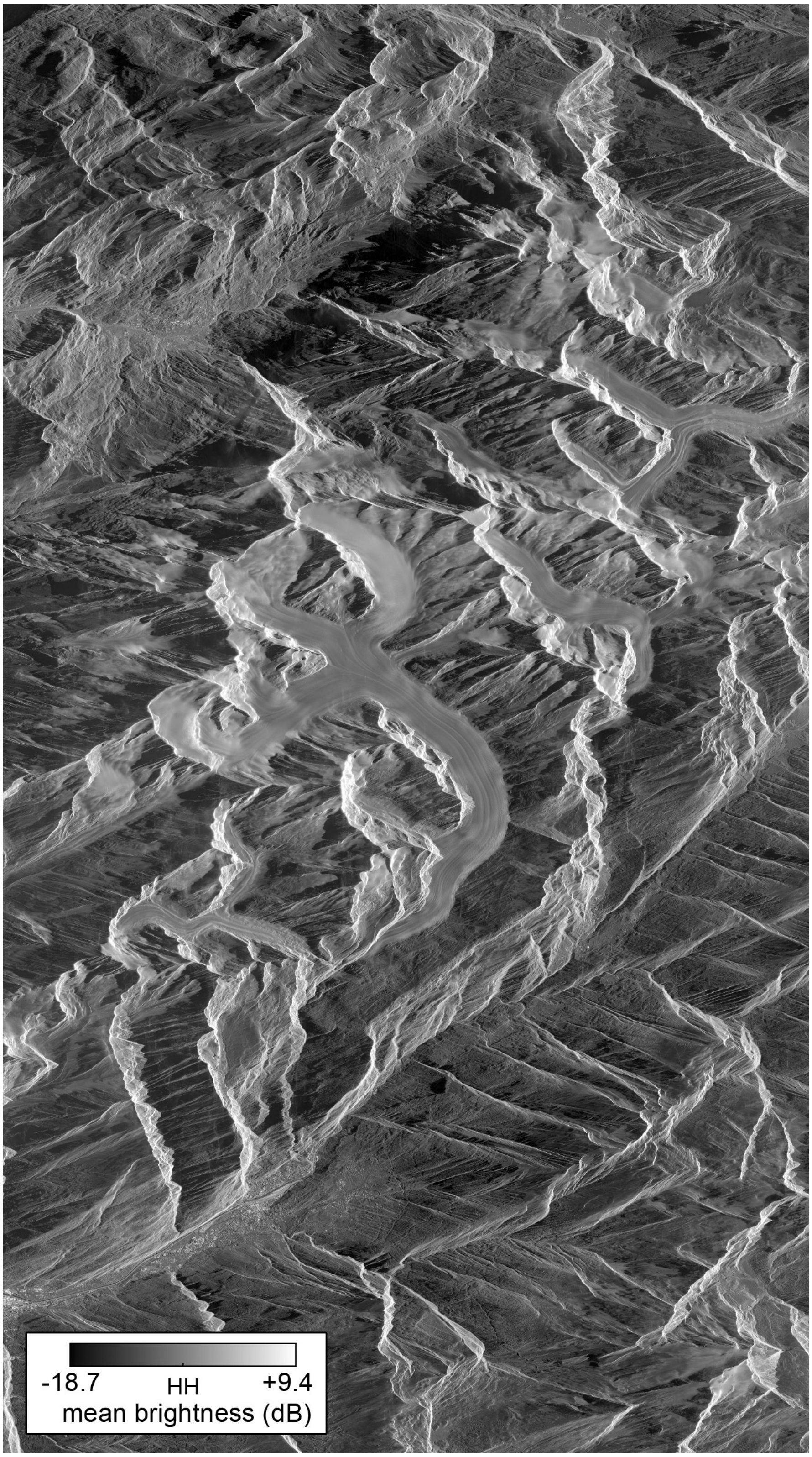

Figure S3. Intensity average of 118 TanDEM-X acquisitions of the Jungfrau-Aletsch region (HH polarization). The image has been flipped/rotated to align approximately with the north-direction. The slant-range direction is from right to left; azimuth from top to bottom.

Figure S4. Backscatter ratio $\hat{I}^{\text{uncal.}}_{\text{r,0,VV}}$ of the mean of 17 scenes (VV) with a baseline $b < 300\,\text{m}$. Narrow areas behind layover with ratios deviating more than 5% from unity might partially result from double-reflections within layover. Some of the dark areas are azimuth ambiguities.

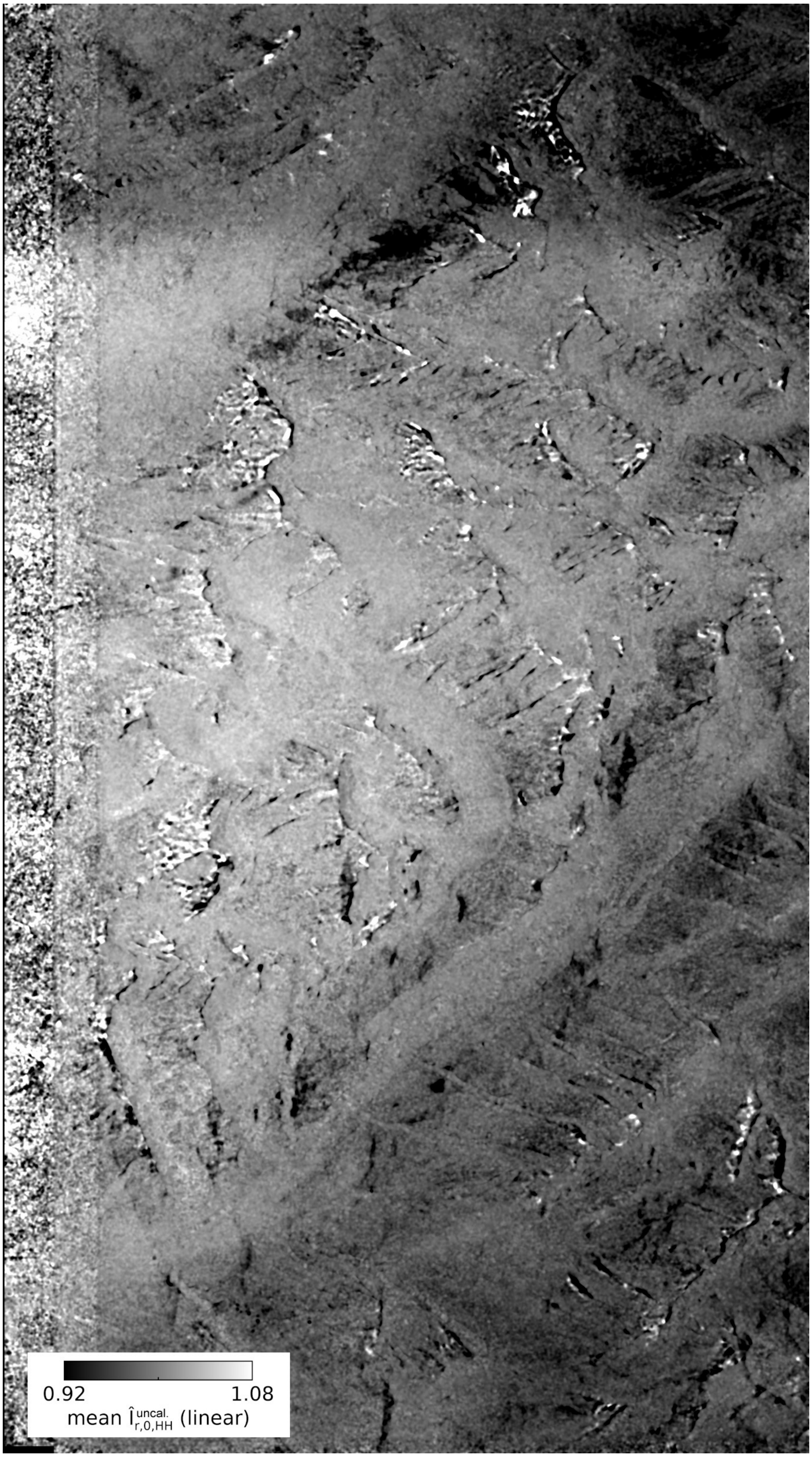

Figure S5. Backscatter ratio $\hat{I}^{\mathrm{uncal.}}_{\mathrm{r,0,HH}}$ of the mean of 17 scenes (HH) with $b < 300\,\mathrm{m}$. The large-scale spatial variations might originate from an uncompensated antenna pattern or different gains. Narrow areas behind layover show values deviating more than 5% from unity (cf. Fig. S4).

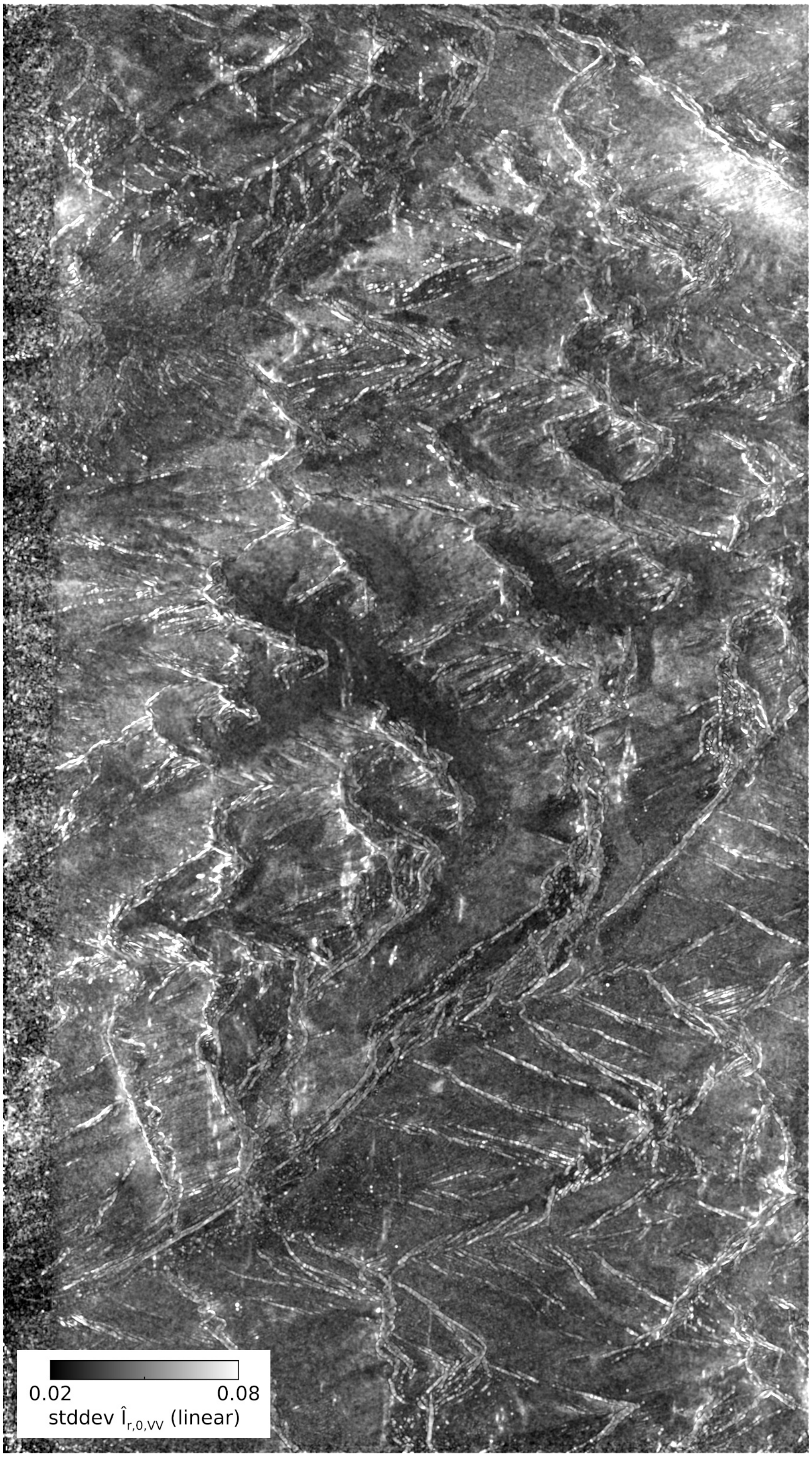

Figure S6. Temporal standard deviation of the backscatter ratio $\hat{I}_{r,0}$ (VV) of all 118 acquisitions after correction for atenna pattern.

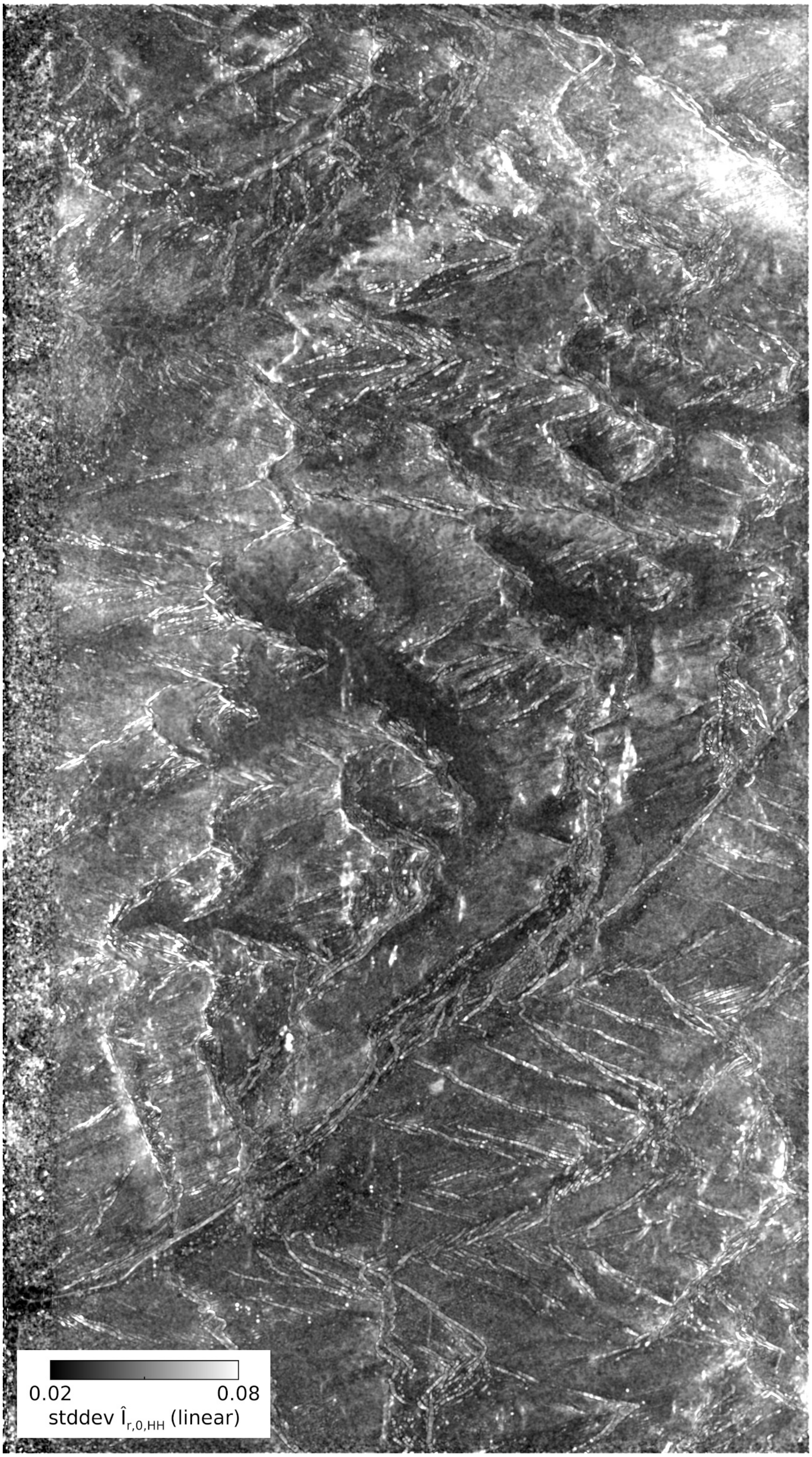

Figure S7. Temporal standard deviation of the backscatter ratio $\hat{I}_{r,0}$ (HH) of all 118 acquisitions after correction for atenna pattern.

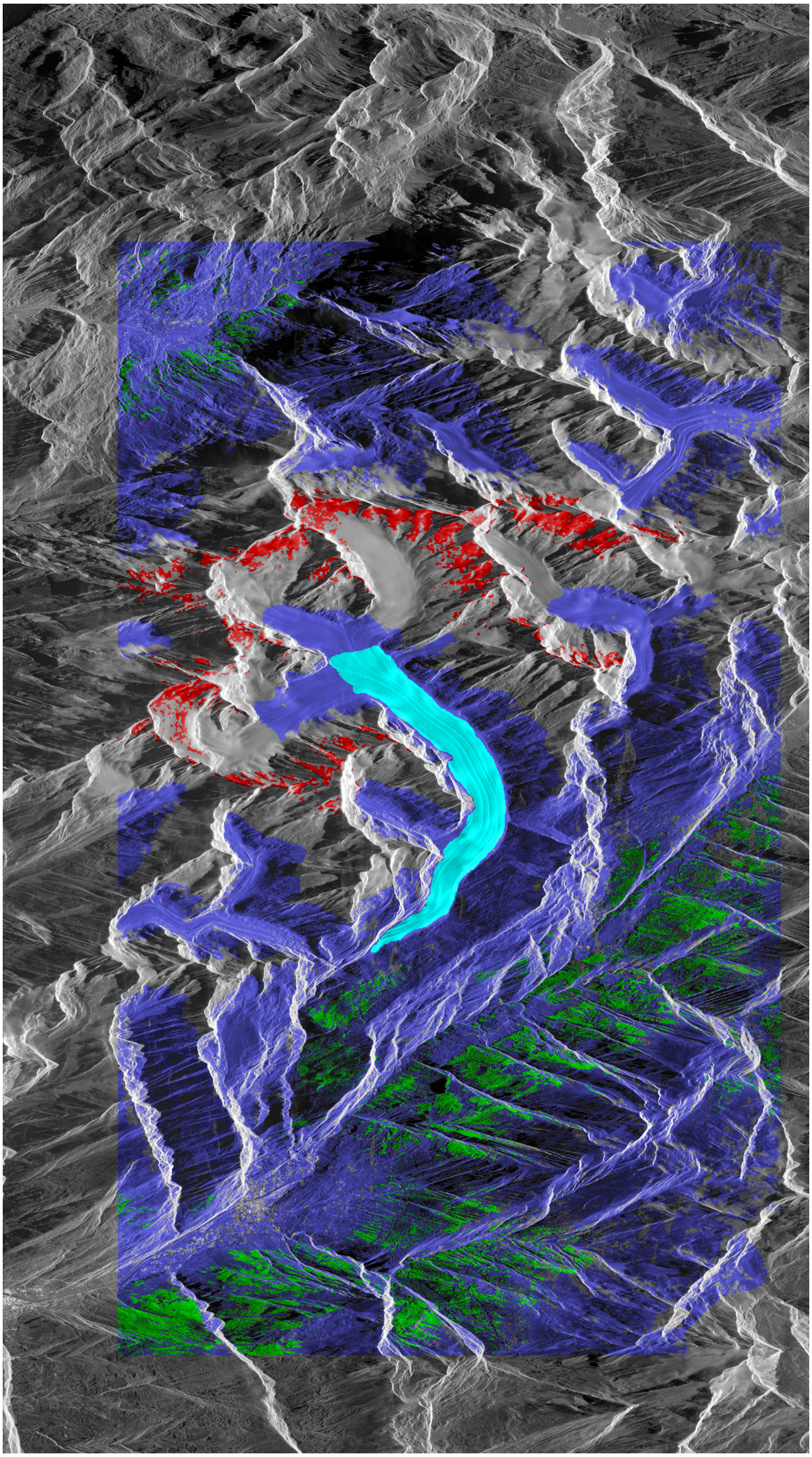

Figure S8. Mask used for the VV polarization indicating the three ROIs, the high accumulation area > 3500 m (red), the ablation area of Great Aletsch Glacier (cyan), and conifer forest (green), together with the mask used for calibration (blue). The masks in HH are very similar.

Additional observation site: Teram-Shehr/Rimo Glacier

On the plateau between Teram-Shehr and Rimo Glacier (35.47°N, 77.30°E), we selected the accumulation area above 6100 m where we expect dry snow that could cause the CBOE. The equilibrium line altitude of Teram-Shehr glacier, an eastern tributary of Siachen glacier in the Karakorum, is at approximately 5250 m (Agarwal et al., 2017). Compared to the Jungfrau-Aletsch dataset, considerably fewer acquisitions are available and, even though the site is closer to the equator, bistatic angles are not significantly larger: for orbit 98 ($\beta = 0.04$–$0.23°$, $\theta = 39°$, asc.) nine acquisitions with high backscatter indicate dry snow and 17 acquisitions with low backscatter indicate wet or partially wet snow. For orbit 75 ($\beta = 0.04$–$0.19°$, $\theta = 43°$, desc.) we found 18 acquisitions indicating dry snow and 25 indicating wet snow. Both datasets are acquired at HH polarization only. To ensure refreezing of snow and firn after summer, we restricted the analysis of the baseline-dependent bistatic-to-monostatic backscatter intensity ratio to data between 01 December and 30 June.

The Teram-Shehr dataset did not provide enough suitable acquisitions for antenna calibration according to Eq. (4) in the main paper. For calibration with Eq. (5), we used the glacier tongue (ablation area, below 5000 m).

Due to the limited amount of acquisitions we only briefly summarize here some observations. In the accumulation area, above 6100 m, we observed backscatter ratios $\hat{I}_{\mathrm{r},0}(\beta)$ between 0.72 and 0.77 in five large-baseline acquisitions with $\beta = 0.193°$ from orbit 75 between 11 May and 24 June 2015 (Fig. S9,top). For orbit 98 with $\beta = 0.231°$, we observed ratios $\hat{I}_{\mathrm{r},0}(\beta)$ between 0.74 and 0.81 between 01 May and 03 June 2015 (Fig. S9,bottom). With Eq. (14) these values allow estimating an lower limit for the backscatter enhancement B_C and correspond to an enhancement of at least 23–39% (+0.9 to +1.4 dB). In comparison, for the Jungfrau-Aletsch region, we obtain a lower limit of 19–27% (+0.8 to +1.0 dB). Due to weak model constraints in the Teram-Shehr dataset, we do not provide parameters estimated by model fits.

Figures S10 and S11 snow that spatially, the enhancement matches to the accumulation area of the Teram-Shehr/Rimo glacier. The periodic variations of visible in the backscatter ratio is already visible on the delivered TanDEM-X CoSSC data and islikely an artifact from the interpolation during coregistration of the bistatic dataset to the monoscatic one.

References

Agarwal, V., Bolch, T., Syes, T. H., Pieczonka, T., Strozzi, T., and Nagaich, R.: Area and mass changes of Siachen Glacier (East Karakoram), Journal of Glaciology, 63, 148–163, https://doi.org/10.1017/jog.2016.127, 2017.

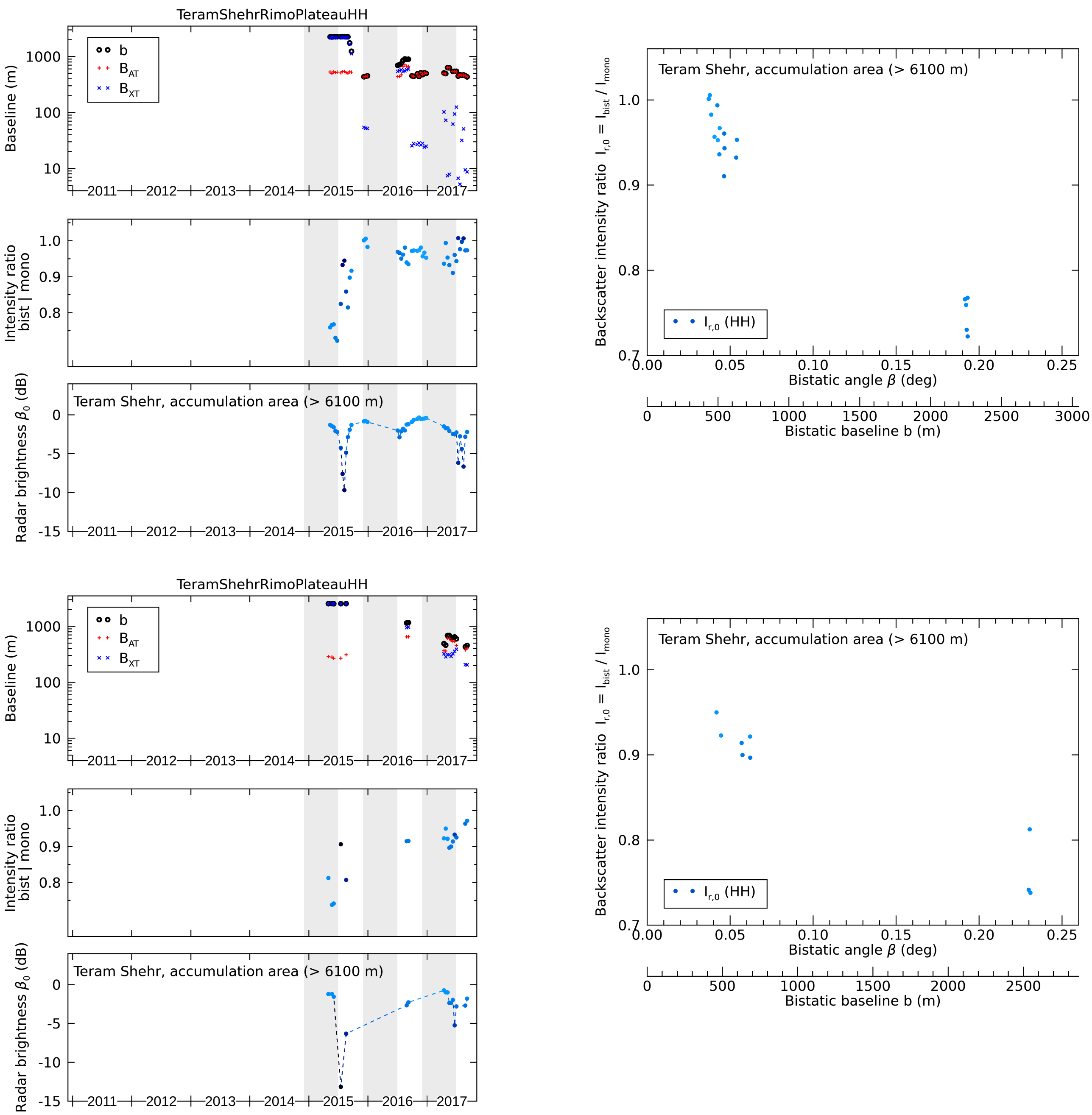

Figure S9. Time series of baselines b, B_{XT}, B_{AT}, bistatic-to-monostatic backscatter ratios $I_{r,0}$, and radar brightness $I_{\mathrm{mono}} \equiv \beta_0$ for the accumulation area of Teram-Shehr glacier in the Karakorum. Top: orbit 075 (descending), bottom: orbit 098 (ascending). The right hand side shows $I_{r,0}$ for dry snow conditions plotted over the bistatic angle β (data only from 01 December - 30 June as indicated by the gray shading in the time-series figures on the left).

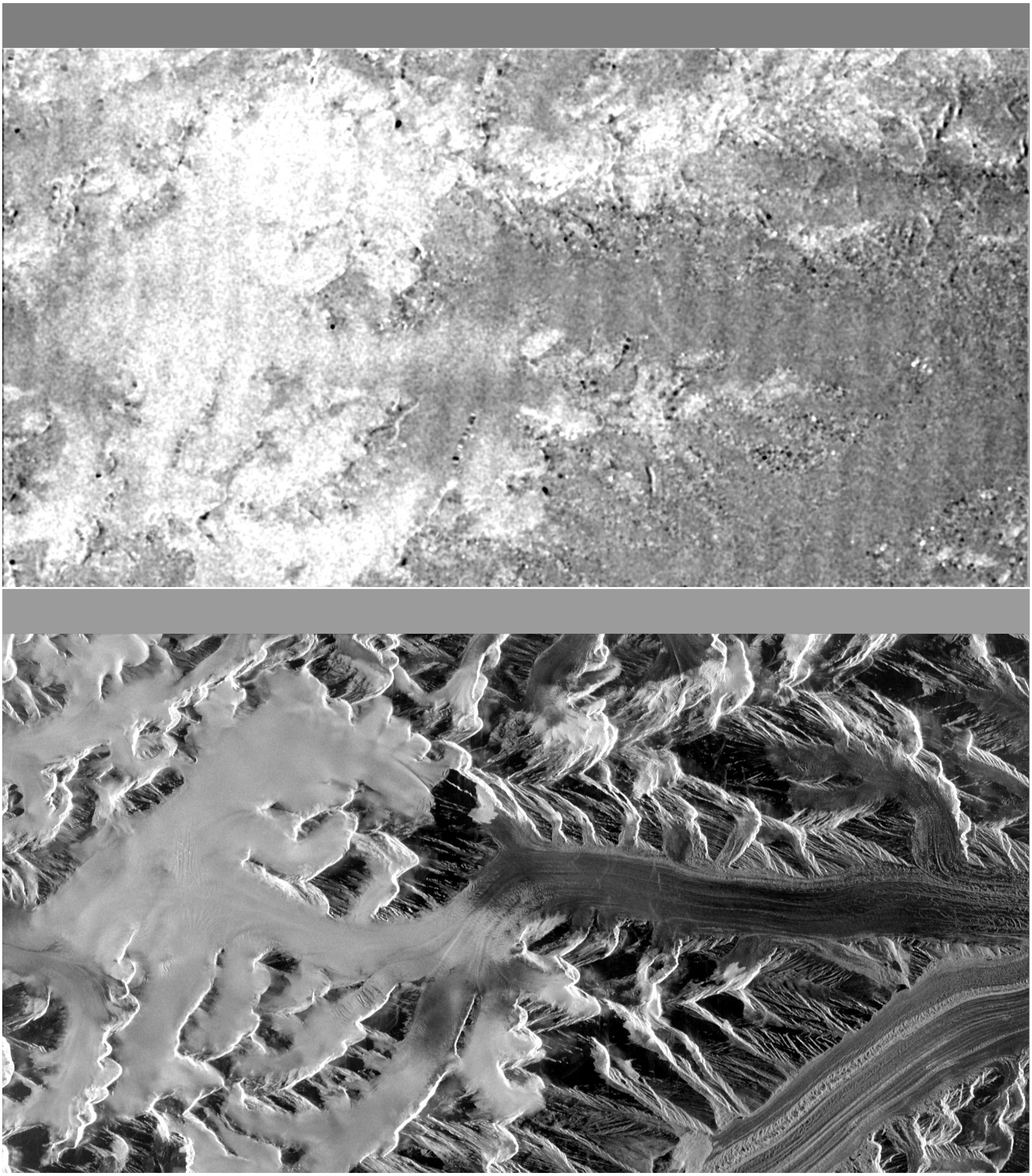

Figure S10. Top: A high monostatic-to-bistatic backscatter ratio $\hat{I}_{r,0}^{-1}$, observed by TanDEM-X on 2015-06-24 (orbit 075, descending) with $\beta = 0.19°$ indicates CBOE in the dry-snow areas. Gray color scale: [-1.5...+1.5 dB]. Bottom: Radar backscatter intensity for the same date. Color scale: [-20..+5 dB]. Bright backscatter indicates dry snow in the accumulation area and dark snow indicates wet snow on the glacier tongue. Images shown in radar coordinates.

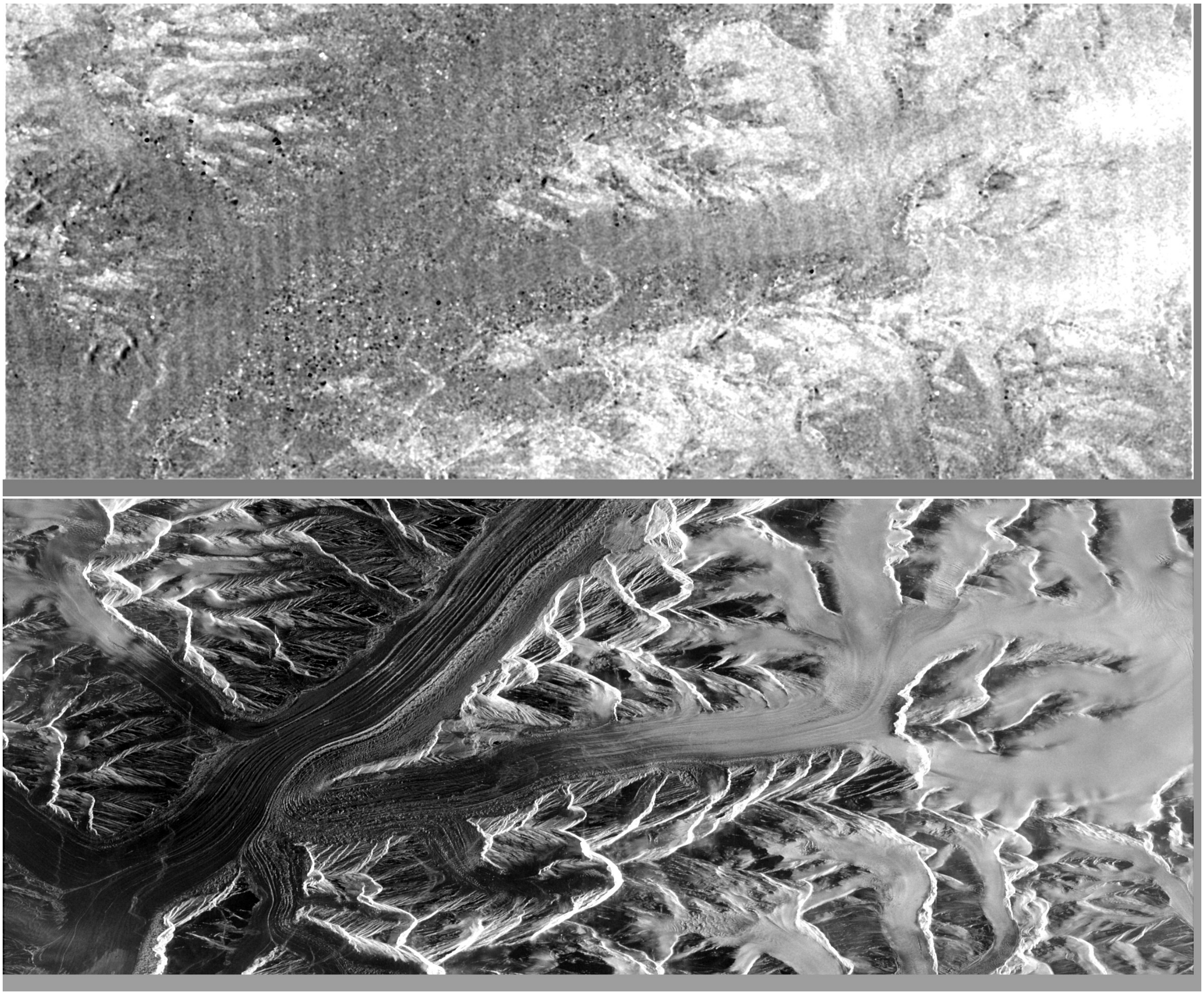

Figure S11. Top: A high monostatic-to-bistatic backscatter ratio $\hat{I}_{r,0}^{-1}$, observed by TanDEM-X on 2015-05-23 (orbit 098, ascending) with $\beta = 0.23^\circ$ indicates CBOE in the dry-snow areas. Gray color scale: [-1.5...+1.5 dB]. Bottom: Radar backscatter intensity for the same date. Colorscale: [-20..+5 dB]. Bright backscatter indicates dry snow in the accumulation area and dark snow indicates wet snow on the glacier tongue. Images shown in radar coordinates.